Chemoselective Transesterification of Methyl (Meth)acrylates Catalyzed by Sodium(I) or Magnesium(II) Aryloxides

Jie Qi Ng,[1] Hiro Arima,[1] Takuya Mochizuki,[1] Kohei Toh,[1] Kai Matsui,[1] Manussada Ratanasak,[2] Jun-ya Hasegawa,*[2] Manabu Hatano,*[3] and Kazuaki Ishihara*[1]

[1]Graduate School of Engineering, Nagoya University, Furo-cho, Chikusa, Nagoya 464-8603, Japan.

[2]Section of Theoretical Catalytic Chemistry, Institute for Catalysis, Hokkaido University, N21W10, Kita-ku, Sapporo, Hokkaido 011-0021, Japan

[3]Graduate School of Pharmaceutical Sciences, Kobe Pharmaceutical University, 4-19-1, Motoyamakitamachi, Higashinada, Kobe 658-8558, Japan

Supporting Information Placeholder

ABSTRACT: A highly chemoselective transesterification of methyl (meth)acrylates catalyzed by sterically demanding 2,6-di-*tert*-butyl-4-methylphenol (BHT)-derived NaOAr or $Mg(OAr)_2$ was developed. The desired transesterification proceeded without undesired Michael additions under mild reaction conditions at 25 °C, and various primary and secondary alcohols, diols, triol, and tetraol on a scale of up to 10 mmol could provide the corresponding functionalized acrylates in high yields. Transition states were proposed based on monomeric and dimeric active species, and computational DFT calculations strongly supported the high chemoselectivity to minimize undesired Michael additions.

KEYWORDS: acrylate, aryloxide, BHT, chemoselectivity, DFT calculations, magnesium, sodium, transesterification

With industrial applications involving heat-resistant adhesives, varnishes, UV-coatings, photoresists, and polymeric plastics, etc., (meth)acrylates are produced on a million-ton scale per year as some of the most important manufactured chemicals.[1] The desirable physical properties of (meth)acrylate polymers, such as flexibility, transparency, and weatherability, can be controlled and fine-tuned by functionalization of the ester group.[2] Therefore, the chemoselective synthesis of various (meth)acrylates is important in this field. In particular, transesterification[3,4] of methyl (meth)acrylates with alcohols is one of the most accessible methods for preparing a variety of desired acrylates, since methyl acrylate **1a** and methyl methacrylate **1b** are inexpensive, commercially available in bulk, and easy to handle as a liquid (i.e., solvent) (Figure 1a). For this purpose, some Lewis acid catalysts can facilitate the desired transesterification. However, at the same time, undesired Michael addition and its initiated polymerization are often observed (Figures 1b and 1c). In particular, **1a** is the simplest acrylate without any substituents, and it is difficult to control the chemoselectivity of transesterification due to its high reactivity and instability regardless of the combined hard or soft alcohols. Therefore, mild reaction conditions with fine-tuned, active, and green sustainable catalysts have been desired, particularly for use in industry.

Considerable attention has been paid to heterogeneous catalysts for use in general transesterification, particularly for biodiesel synthesis, which would offer the industrial advantages of less harmful processes and the possibility of

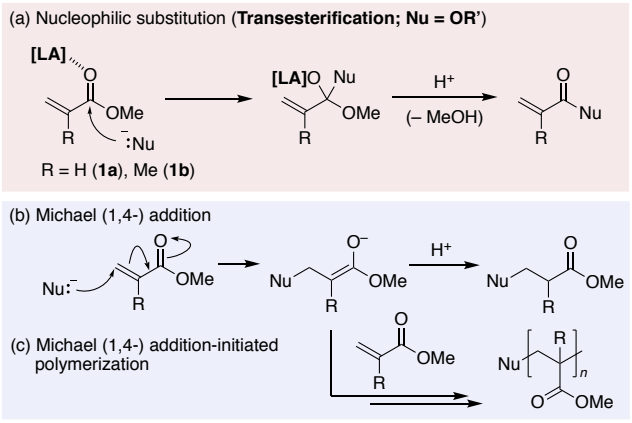

Figure 1. Chemoselective transesterification of methyl (meth)acrylates **1a** and **1b**. (a) Nucleophilic substitution (transesterification). (b) Michael addition. (c) Michael addition-initiated polymerization.

recycling.[5] Nevertheless, there are still only a few of examples of the transesterification of (meth)acrylates, such as with silica-supported Zr(IV)[6a] and Ti(IV)[6b] catalysts, polystyrene-supported Ti(IV) catalysts,[6c] aluminium oxide (Al_2O_3)-supported Ca(II) catalysts,[6d] etc., for which their inherently low catalytic activity still requires heating conditions and a long reaction time (typically 70–90 °C for 6–24 h). On the other hand, there are

still only a few examples of homogeneous catalysts. One of the most striking developments is a zinc(II) cluster catalyst, $Zn_4(OCOCF_3)_6O$,[7] which was reported by Ohshima and co-workers in 2016 (Scheme 1a).[8] In their paper, reactions with **1a** and **1b** were carried out with the use of $Zn_4(OCOCF_3)_6O$ (5 mol% based on Zn(II)) and 4-(dimethyl-amino)pyridine (DMAP) (20 mol%) at 60–80 °C for 24–48 h. Although secondary alcohols were not used, the corresponding primary alcohol-derived (meth)acrylates were obtained in high to excellent yields. In 2018, our group also reported the transesterification of **1b** with the use of a green sustainable ammonium catalyst $[Me_4N]^+[OCO_2Me]^-$ (**8**) at 100 °C, which could provide not only the corresponding primary but also the corresponding secondary alcohol-derived methacrylates in high to excellent yields (Scheme 1b).[9] Unfortunately, however, the system could not be used for the transesterification of **1a** with benzyl alcohol **2a** even at a reduced temperature (70 °C), and **3a** was obtained in 26% yield along with undesired byproducts **4a** (10%), **5a** (1%), **6a** (18%), and **7a** (1%) (Scheme 1c).

Scheme 1. Reported homogeneous catalysts for (meth)acrylate synthesis and our early study using $[Me_4N]^+[OCO_2Me]^-$.

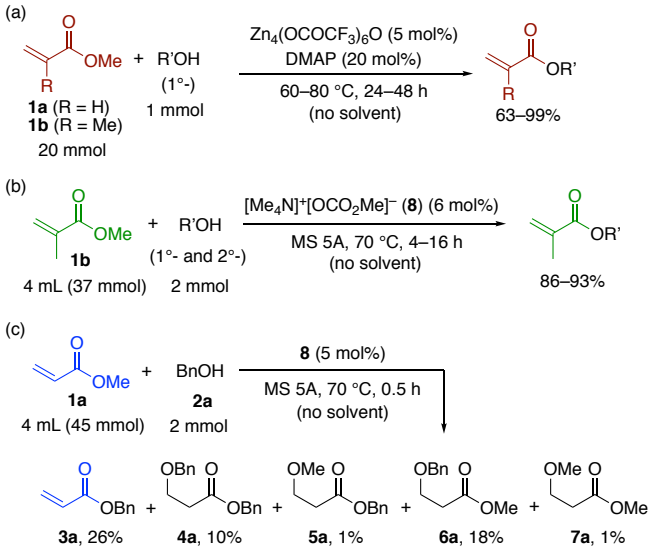

In such a situation, we were interested in sodium(I) and magnesium(II) salts of 2,6-di-*tert*-butyl-4-methylphenol (BHT) (**9** and **10**), which have been reported to be highly efficient in the ring-opening polymerization (ROP) of cyclic esters (Figure 2a).[10] Remarkably, the **9**- or **10**-catalyzed ROP reactions proceeded smoothly even at 25 °C within 1 h. In particular, among other phenol candidates,[11] sterically demanding BHT-salts have been commonly used in this reaction due to the high catalytic activity of monomeric species[10] along with their commercial availability, chemical stability against oxidation,[12] and low toxicity of BHT.[13] Of course, alkali and alkaline earth metal ions are abundant and non-toxic,[14] and thus **9** and **10** are highly attractive as possible catalysts for the present chemoselective transesterification of methyl (meth)acrylates. In particular, we envisioned that **9** and **10** could serve as acid–base cooperative catalysts, which can activate both **1a**/**1b** and alcohol *via* conformations with a four/four-membered ring, without the generation of Michael addition-derivatives (Figure 2b).

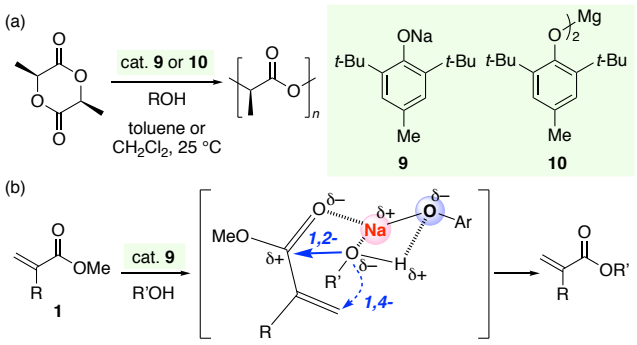

Figure 2. BHT-derived sodium(I) and magnesium(II) aryloxide catalysts. (a) The ring-opening polymerization of cyclic esters. (b) The present chemoselective transesterification of (meth)acrylates.

We initiated our exploration by attempting the transesterification of problematic methyl acrylate **1a** with simple and highly reactive benzyl alcohol **2a** as a probe reaction at 25 °C for 30 min in the presence of $Cu(CS_2NMe_2)_2$ (0.2 mol%) as a polymerization inhibitor (Table 1). Due to a general industrial practice, bulk-supplied inexpensive **1a** was used as a solvent. To identify better conditions, the reactions were intentionally carried out in the absence of molecular sieve (MS) 5A, since removal of methanol by MS 5A would suppress undesired byproducts **5a**, **6a**, and **7a** to some extent. First, BHT-derived alkali and

Table 1. Screening of catalysts for the transesterification of 1a with benzyl alcohol (2a).[a]

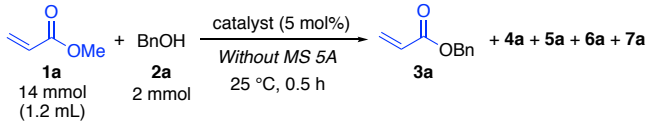

entry	catalyst	yield (%)[b]				
		3a	**4a**	**5a**	**6a**	**7a**
1	LiOAr	50	8	8	25	13
2	NaOAr (**9**)	49	8	0	38	55
3	KOAr	40	8	2	47	45
4	$Mg(OAr)_2$ (**10**)	**40**	**0**	**0**	**0**	**1**
5[c]	**10**	**70**	**0**	**0**	**1**	**4**
6	$Ca(OAr)_2$	6	0	0	1	1
7	NaOMe	43	8	1	41	40
8	KO*t*-Bu	20	10	17	30	30
9	$Mg(Ot\text{-}Bu)_2$	60	1	0	8	15
10[c]	$Ca(Oi\text{-}Pr)_2$	40	1	0	8	15
11[c]	$Ti(On\text{-}Bu)_4$	0	0	0	0	0
12[c]	$Fe(OEt)_3$	0	0	0	0	0
13[c]	$Zn(OMe)_2$	0	0	0	0	0
14	$La(Oi\text{-}Pr)_3$	62	5	10	18	32
15	$[Me_4N]^+[OCO_2Me]^-$ (**8**)	2	0	0	1	0
16	$[Me_4N]^+[OAr]^-$	34	10	0	54	42

[a] The reaction was carried out with **1a** (14 mmol), **2a** (2 mmol), catalyst (5 mol%), and $Cu(CS_2NMe_2)_2$ (polymerization inhibitor, 0.2 mol%) at 25 °C unless noted otherwise. ArOH is BHT. [b] Isolated yield as a mixture. The ratio was determined by ^1H NMR. The sum of the product yields could be exceeded 100%, since **7a** was generated from excess **1a**. [c] Reaction time was 3 h.

alkaline earth metal aryloxides, which we were interested in,[15] were examined (entries 1–6). As a result, $Mg(OAr)_2$ (**10**) showed much better chemoselectivity than LiOAr, NaOAr (**9**), and KOAr, and **3a** was obtained almost exclusively in 40% yield (entry 4). A prolonged reaction time of up to 3 h with the use of **10** could provide **3a** in 70% yield with high chemoselectivity, although the reaction was almost established at that time due to the equilibrium regarding **2a** and methanol in the absence of MS 5A (entry 5). In sharp contrast to Mg(II) catalyst **10**, $Ca(OAr)_2$ showed low catalytic activity with unimpressive chemoselectivity, partially due to its low solubility (entry 6). Moreover, other commercially available metal alkoxides, such as alkali and alkaline earth metal salts,[3] Ti(IV),[16] Fe(III),[17] Zn(II),[7,8] and La(III)[18] salts, which have been known to promote general transesterification reactions, were examined (entries 7–14). However, significant amounts of byproducts **4a**, **5a**, **6a**, and **7a** were generated along with desired **3a**, and the chemoselectivity was not impressive. $Mg(O\textit{t}\text{-Bu})_2$ was more reactive but less effective than **10**, and **6a** and **7a** were obtained along with desired **3a** (60% yield) (entry 9). $Ca(O\textit{i}\text{-Pr})_2$ showed low catalytic activity and $Ti(O\textit{n}\text{-Bu})_4$, $Fe(OEt)_3$, and $Zn(OMe)_2$ showed no catalytic activity under the mild reaction conditions at 25 °C within 3 h (entries 10–13). Our previous catalyst $La(O\textit{i}\text{-Pr})_3$ gave **3a** in 62% yield, but significant amounts of the byproducts **4a**, **5a**, **6a**, and **7a** were generated (entry 14). Moreover, as expected, $[Me_4N]^+[OCO_2Me]^-$ (**8**) showed low catalytic activity at 25 °C due to the slow initial *in situ* formation of active species $[Me_4N]^+[OBn]^-$ through the release of CO_2 and methanol (entry 15). Instead, $[Me_4N]^+[OAr]^-$ improved the activity, and **3a** was obtained in 34% yield along with significant amounts of **4a**, **6a**, and **7a** (entry 16). From these screenings, we found that the central metal and aryloxide would be important for controlling the chemoselectivity in the present reaction.

Since Mg(II) catalyst **10** was useful for the transesterification of **1a** with **2a**, the substrate scope was examined in the presence of MS 5A, which should effectively remove methanol (Scheme 2). As expected, **3a** was obtained in quantitative yield at 25 °C within 30 min. The same reaction was scalable with a reduced amount of catalyst such as 0.5 mol%, and 1.62 g of **3a** was obtained quantitatively (Scheme 3). Other primary alcohols could be used, and an array of structural motifs, such as a heteroaromatic group (**3b**), long hydrocarbon chain (**3c**), unsaturated hydrocarbon chain (**3d**), (–)-myrtenol derivative (**3e**), and α-galactopyranose derivative (**3f**) were successfully synthesized in more than 99% yield. Remarkably, sterically more-hindered secondary alcohols were also available, although a prolonged reaction time was typically required, and the monomers for synthetic resins, such as 5-nonanyl acrylate **3g** (94% yield for 24 h), isobornyl acrylate **3h** (83% yield for 24 h), and (–)-menthyl acrylate **3i** (90% yield for 48 h) as a typical pressure-sensitive adhesive were obtained. Moreover, cholesteryl acrylate **3j** was obtained in 70% yield within 24 h, although an elevated temperature of 60 °C was required due to low reactivity and low solubility. It should be noted that, even at the high temperature, no undesirable byproducts were obtained, and the remaining starting materials were recovered. Unfortunately, although catalyst **10** could not be recovered as it was, stable BHT could be recovered every time in 95–99% yield through a routine workup procedure by silica gel column chromatography.

Scheme 2. Transesterification of 1a with various alcohols 2.[a]

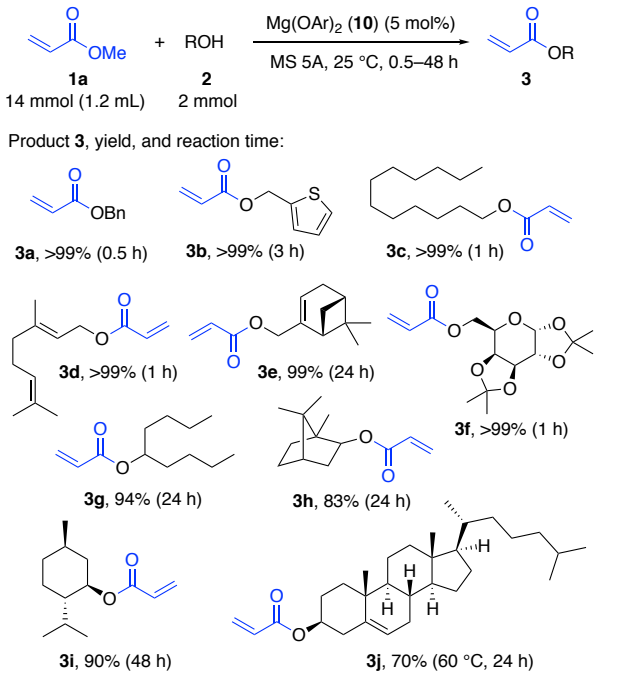

[a] The reaction was carried out with **1a** (14 mmol), **2** (2 mmol), **10** (5 mol%), $Cu(CS_2NMe_2)_2$ (polymerization inhibitor, 0.2 mol%), and MS 5A (0.4 g) at 25 °C unless noted otherwise. Isolated yields after flash silica gel column chromatography are shown.

Scheme 3. Scale-up synthesis of 3a.

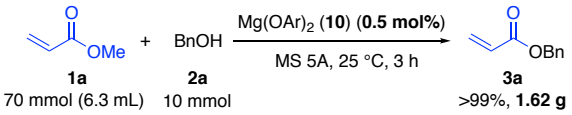

Next, we extended our catalytic system to cover the chemoselective transesterification of methyl methacrylate **1b** instead of **1a** in the presence of 4-acetamido-TEMPO (0.1 mol%) as a polymerization inhibitor (Scheme 4). However, Mg(II) catalyst **10** showed rather low catalytic activity for the reaction between **1b** and **2a**, and it took 6 h to complete the reaction, although excellent chemoselectivity for **11a** was observed (see brackets b). Moreover, **10** was ineffective for bulky secondary alcohols, and the corresponding products **11b** and **11c** were scarcely obtained even after 24 h, although any side products were not obtained. After taking into account the expected chemical stability of **1b**, unlike reactive **1a**, we examined more active alkali metal catalysts. As a result, even though the catalyst loading was reduced to 2.5 mol%, NaOAr (**9**) was much more effective than the others (see the Supporting Information), and **11a**, **11b**, and **11c** were respectively obtained in 95–>99% yields without any byproducts within a greatly reduced reaction time (0.5–3 h) at 25 °C. Remarkably, the reaction of **1b** and **2a** proceeded quantitatively with the use of even 0.5 mol% of **9**. With the optimized catalyst for **1a** in hand, a wide substrate scope was disclosed. Primary alcohols provided the corresponding products **11d–j** in 93–>99% yields within 0.5–1 h. In particular, whereas highly chelative substrates and/or products

Scheme 4. Transesterification of 1b with various alcohols 2.[a]

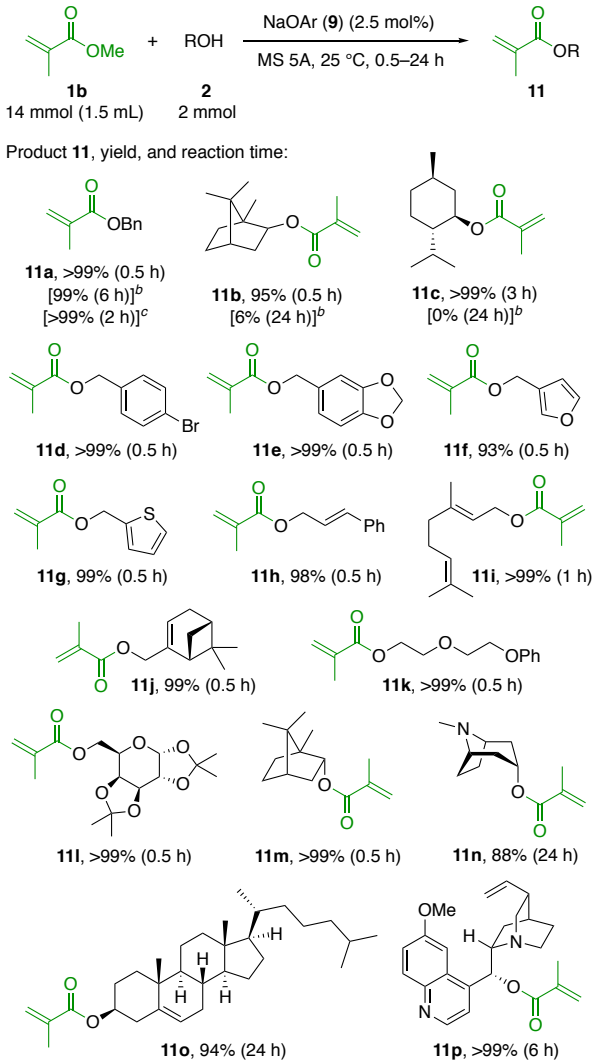

[a] The reaction was carried out with **1b** (14 mmol), **2** (2 mmol), **9** (2.5 mol%), 4-acetamido-TEMPO (polymerization inhibitor, 0.1 mol%), and MS 5A (0.4 g) at 25 °C unless noted otherwise. Isolated yields after flash silica gel column chromatography are shown. [b] The reaction was carried out with **10** (5 mol%) in place of **9** (2.5 mol%). [c] 0.5 mol% of **9** was used.

often deactivate catalysts, heteroaromatic acrylates **11e** and **11g**, allylic acrylates **11h** and **11i**, and diethylene glycol-derived acrylate **11k** could be obtained successfully. Moreover, functionalized bulky secondary alcohols could also be used, and α-galactopyranose derivative **11l**, bornyl methacrylate **11m**, tropinyl methacrylate **11n**, cholesteryl acrylate **11o**, and quinine methacrylate **11p** were obtained in 88–>99% yields with excellent chemoselectivity. In all cases in Scheme 4 as well as Scheme 2, BHT could be almost fully recovered through flash silica gel column chromatography.

Unstable (meth)acrylate synthesis is a challenge,[19] and a few examples were demonstrated (Scheme 5). Allyl methacrylate **13a** and glycidyl methacrylate **13b**, which are chelative and particularly susceptible to nucleophilic attack and thus sometimes result in decomposition and polymerization,[20] could be obtained in 90% and 76% yield, respectively. Trifluoroethyl

Scheme 5. Synthesis of unstable (meth)acrylates.[a]

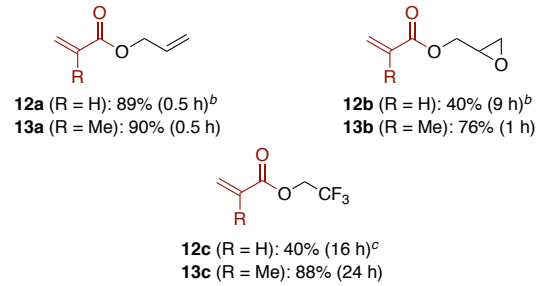

[a] Reaction was carried out with **1a** or **1b** (14 mmol), **2** (2 mmol), **9** (2.5 mol%), polymerization inhibitor (0.2 mol%), and MS 5A (0.4 g) at 25 °C unless noted otherwise. [b] 5 mol% of **9** was used at –20 °C. [c] 5 mol% of **9** was used at 25 °C.

methacrylate **13c**, which is also unstable due to its electron-withdrawing nature,[21] was also obtained in 88% yield. Unfortunately, these corresponding acrylates **12a–c** could not be obtained by using less active Mg(II) catalyst **10** since no reaction occurred, but much more active Na(I) catalyst **9** could be used at –20 °C to suppress undesired side reactions. As a result, **12a–c** could be provided with excellent chemoselectivity, although the yields were moderate to good.

Moreover, the efficiency of our catalyst system at 25 °C was especially highlighted by the industrially useful diol-, triol-, and tetraol-derived (meth)acrylate synthesis (Scheme 6). Mg(II) catalyst **10** was effective for the transesterification of **1a** with

Scheme 6. Transesterification with diols, triol, and tetraol.[a]

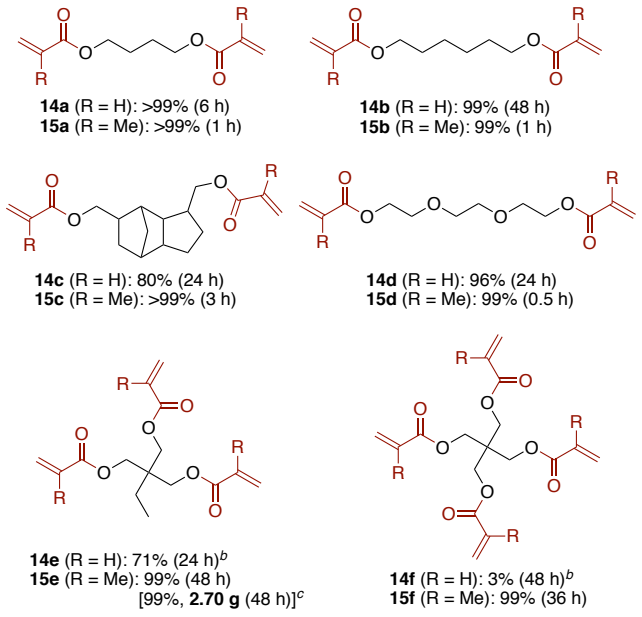

[a] Reaction was carried out with **1a** (14 mmol), **2** (2 mmol), **10** (5 mol%), $Cu(CS_2NMe_2)_2$ (polymerization inhibitor, 0.2 mol%), and MS 5A (0.4 g), or **1b** (14 mmol), **2** (2 mmol), **9** (5 mol%), 4-acetamido-TEMPO (polymerization inhibitor, 0.1 mol%), and MS 5A (0.4 g) at 25 °C unless noted otherwise. [b] Reaction temperature was 60 °C. [c] Triol (10 mmol), **1b** (12 mL), **9** (5 mol%), 4-acetamido-TEMPO (polymerization inhibitor, 0.1 mol%), and MS 5A (2.4 g) were used.

diols, and the corresponding linear alkyl chain acrylates **14a** and **14b**, structurally rigid hexahydromethanoindan-derived acrylate **14c**, and highly chelative triethylene glycol-derived acrylate **14d** were obtained. Additionally, the relevant methacrylates **15a**–**d** were obtained almost quantitatively with the use of Na(I) catalyst **9**. Remarkably, a successful transesterification of trimethylolpropane could be performed, and tri(meth)acrylates **14e** (71% yield) and **15e** (99% yield) were obtained. Notably, the gram-scale synthesis provided **15e** in 99% yield (2.70 g) without serious problems. Pentaerythritol, as an industrially important tetraol, could be converted to the corresponding methacrylate **15f** quantitatively, although the corresponding acrylate **14f** was hardly obtained (up to 3% yield). For the synthesis of **14f**, catalysis with **9** at –20 °C for 24 h was also ineffective.

Despite the industrial importance of unsymmetrical α,ω-diol-derived crosslinkable bis-(meth)acrylate monomers in electronic, coating, and photoresist materials, control of the chemoselective reaction is difficult due to reversible intramolecular transesterification. However, by taking advantage of such intramolecular transesterification, we could smoothly react the low-reactive ω-tertiary alcohol moiety with the α-(meth)acrylate moiety. In this regard, we could control the chemoselective mono- and di-transesterification of unsymmetrical 1,3-diol **16** by using Mg(II) catalyst **10** and Na(I) catalyst **9**, respectively (Scheme 7). With 5 mol% of **10**, mono-(meth)acrylates **17a** and **17b** were obtained quantitatively. On the other hand, with 5 mol% of active **9**, which could facilitate

Scheme 7. Selective mono- and di-transesterification with unsymmetrical 1°/3°-diol 16.

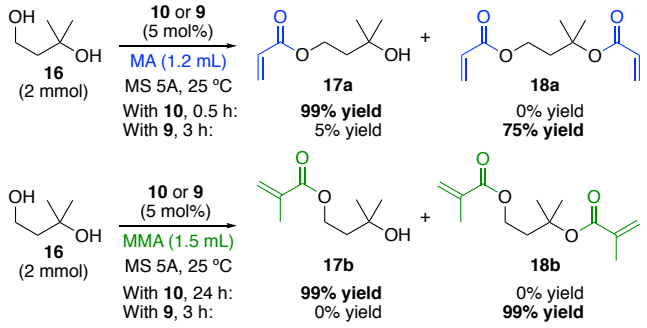

Scheme 8. Transesterification of other conjugated esters.[a]

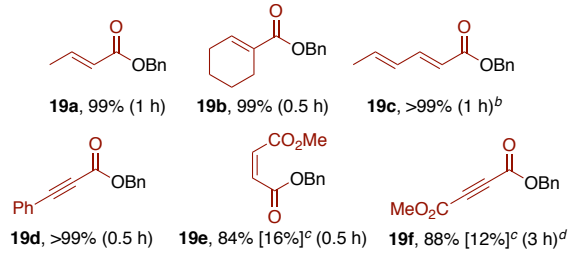

[a] Reaction was carried out with conjugated methyl ester (14 mmol), **2** (2 mmol), **9** (2.5 mol%), and MS 5A (0.4 g) at 25 °C unless noted otherwise. [b] Ethyl ester was used as a starting substrate. [c] Data in brackets are the yield of Michael adducts. [d] 5 mol% of **9** was used, and reaction temperature was –20 °C.

intramolecular transesterification with the low-reactive tertiary alcohol moiety, di-(meth)acrylates **18a** and **18b** were obtained in respective yields of 75% and 99%.

In place of **1a** and **1b**, other conjugated esters were used in the present catalysis (Scheme 8). As a result, with the use of 2.5 mol% of Na(I) catalyst **9** at 25 °C, crotonate **19a** and cyclohexenecarboxylate **19b** were successfully obtained in quantitative yields. Moreover, 1,3-diene conjugated ester **19c** was obtained in >99% yield from the commercially available ethyl ester. Conjugated alkynyl ester **19d** was also obtained quantitatively. Selective single transesterification of conjugated diesters, which are very strong Michael acceptors, was also applicable at –20 °C, and the corresponding maleate **19e** and acetylenedicarboxylate **19f** were obtained while minimizing undesired Michael additions.

Finally, we turned our attention to mechanistic aspects. According to the literature on ring-opening polymerization of cyclic esters,[10] BHT-derived sterically demanding sodium(I) and magnesium(II) aryloxides provide monomeric species in coordinative solvents.[22] In our present study,[23] since coordinative **1a** and **1b** were used as solvents, we proposed possible monomeric transition states TS-**20** and TS-**21** with four-coordinated pseudo-tetrahedral geometries as shown in Figure 3. In these transition states, methyl (meth)acrylate and alcohol (ROH) are coordinated to the acidic Na(I) or Mg(II) center. At the same time, due to the inherent basic nature of alkali and alkaline earth metal aryloxides, alcohol would exhibit hydrogen bonding to the OAr moiety to make a four-membered ring.[10,22] Based on such acid–base cooperative activation, methyl (meth)acrylate and alcohol are brought into close proximity for the relatively tight transition states involving the corresponding four/four-membered ring as shown in TS-**20** and TS-**21**. Compared to TS-**21**, TS-**20** is sterically demanding due to two aryloxide moieties. Consequently, the sterically restricted methyl acrylate **1a** would reasonably avoid an undesired Michael addition reaction pathway, when bulky complex **10** was used as a catalyst. Since NaOAr **9** with the sole aryloxide moiety does not have such constraints like $Mg(OAr)_2$ **10**, poor chemoselectivity would be observed in the reaction of **1a** (see Table 1). Instead, since less sterically demanding **9** would have higher catalytic activity than **10**, methyl methacrylate **1b**, which is much less problematic than **1a** for the undesired Michael addition, could be used successfully. In other words, sterically demanding and thus less

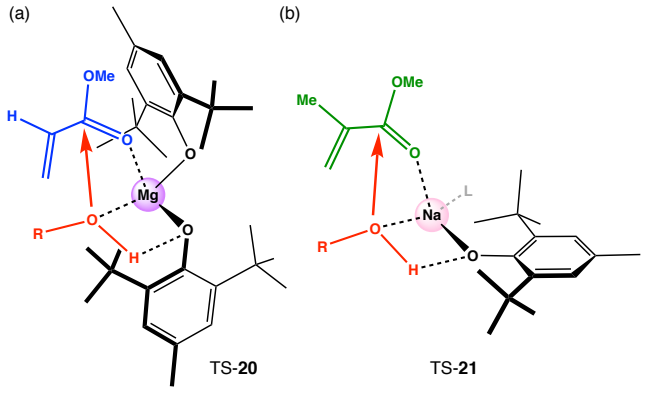

Figure 3. Possible transition states. L = ester or alcohol. (a) TS-**20** based on the monomeric **10** complex. (b) TS-**21** based on the monomeric **9** complex.

active **10** would not be suitable for **1b**, which is inherently less reactive than **1a**. Overall, the matched respective combination of **9** for **1a** and **10** for **1b** would be reasonably explained.

To numerically verify the mechanistic considerations, DFT calculations were performed for the transesterification of **1a** with **2a** catalyzed by **10**. The results were compared to those for Michael addition of the same substrates. For computational details, see section 16 in the SI. Before investigating the reaction pathway, we studied the relative stability of *s-trans*- and *s-cis*-isomers of **1a** by DFT calculation. As shown in Figure S4 in the SI, the *s-cis*-isomer is more stable than the *s-trans*-isomer by 0.7 kcal/mol. These *s-cis*- and *s-trans*-conformations were interconvertible with an activation energy of about 5 kcal/mol. Assuming thermodynamic equilibrium, 70% of **1a** would be in

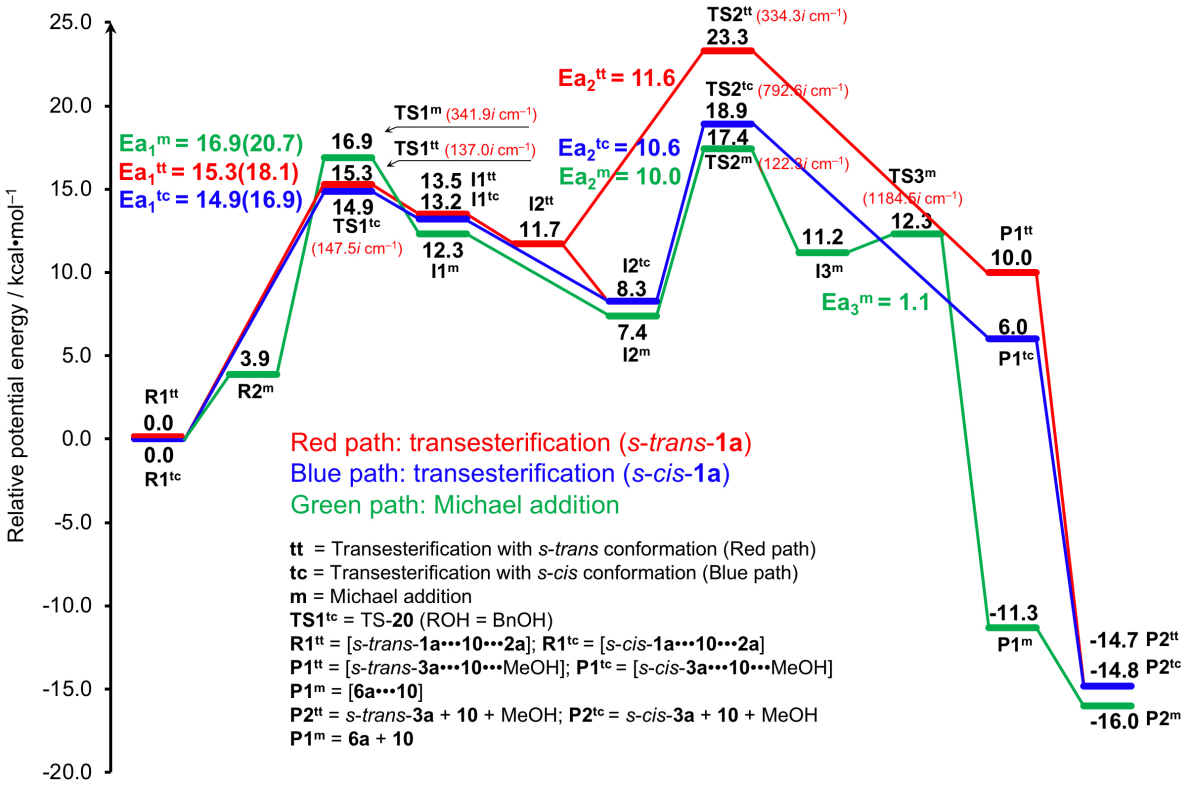

Figure 4. Potential energy profile for transesterification and Michael addition of **1a** with **2a** using the Mg(II) catalyst **10**. For transition states, imaginary frequencies are given in parentheses. For rate determining steps, activation free energy, $\Delta G^{\ddagger}$, is shown in parenthesis.

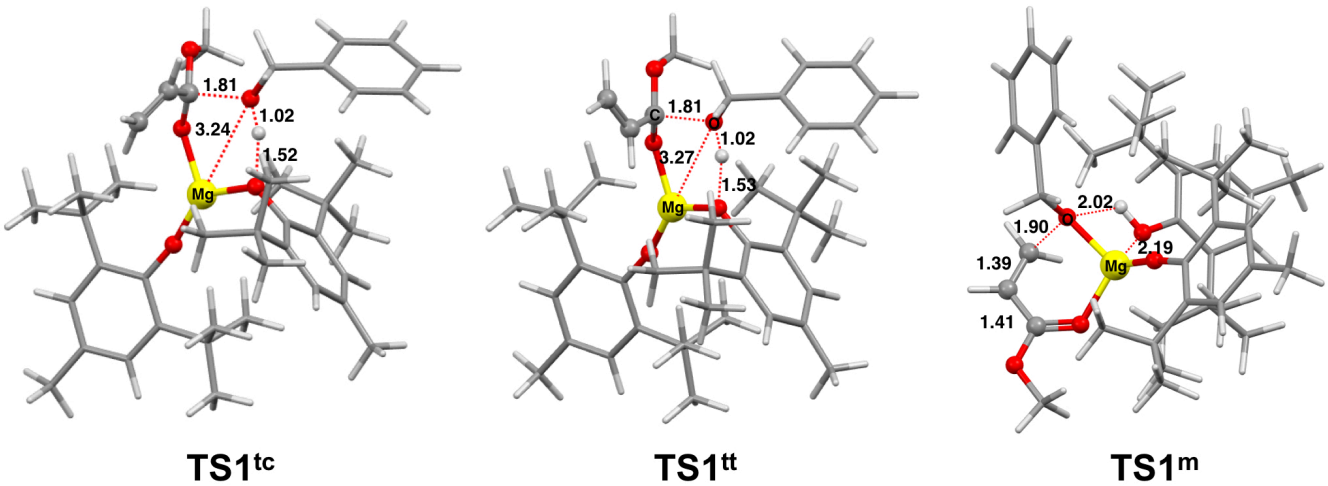

Figure 5. Optimized structures of **TS1**^{tc}, **TS1**^{tt}, and **TS1**^{m}. Bond lengths are given in Å.

a *cis*-conformation according to the Boltzmann distribution. The calculated energy deviation is so small that the reaction pathways for both *s-cis*- and *s-trans*-cases were investigated. The calculated potential energy profile is shown in Figure 4, and the structures of some key transition states are also shown in Figure 5. Other optimized structures are also shown in section S16 of the SI.

First, the potential energy profile for the transesterification of *s-cis*-**1a** is explained. This pathway is the most plausible among the three pathways investigated in the present study. The reactant state **R1^{tc}** with *s-cis*-**1a** was slightly, albeit negligibly, more stable than **R1^{tt}** with *s-trans*-**1a**. A nucleophilic attack by **2a** leads to transition state **TS1^{tc}** (for structure, see Figure 5), which corresponds to TS-**20** with a four/four-membered ring. This is the rate-determining step, and the calculated activation energy is 14.9 kcal/mol. The TS relaxes by 1.7 kcal/mol to an intermediate state **I1^{tc}**. This elementary step includes both C–O formation and proton transfer from **2a** to OAr in a concerted manner. A further relaxation could happen in the intermediate state and lead to the **I2^{tc}** state where ArOH donates a hydrogen bond to the oxygen atom of a methoxy group. This intermediate state is connected to **TS2^{tc}** and then to **P1^{tc}** state. This step is also a concerted reaction where a methoxy group is eliminated and accepts a proton in a concerted mechanism. The calculated activation energy is 10.6 kcal/mol. In this **P1^{tc}** state, generated MeOH is not properly coordinated to the Mg center. Another structural relaxation could lead to the most stable **P2^{tc}** state.

The potential energy profile for the *s-trans*-**1a** case was compared to that for the *s-cis* case. As seen in Figure 4, the profile shown by red lines is very similar until the intermediate state **I1^{tt}**. The structure of transition state **TS1^{tt}** also showed a four/four-membered ring conformation. The calculated activation energy for **TS1^{tt}** is 15.3 kcal/mol, which is comparable to that in the *cis* case. However, the intermediate state **I2^{tt}** is less relaxed than the **I2^{tc}** state in the *cis*-pathway. The transition state **TS2^{tt}** also follows the same trend. As seen in Figure S6 in the SI, the O=C–C=C dihedral angles in **I2^{tt}** and **TS2^{tt}** are not planar due to intramolecular steric repulsion with the methoxy group. This repulsion arises from the hydrogen bond between ArOH and the oxygen atom of the methoxy group. This hydrogen bond restricts the orientation of the methyl group in the direction of the C=C skeleton. However, once the *s-trans*-conformation is relaxed to the *s-cis* form (**I2^{tc}**), the *s-trans*-pathway intersects with the *s-cis*-pathway. Therefore, the *s-trans*-pathway is also expected to be one of the active pathways.

The Michael addition pathway was compared with the transesterification pathways. The **R2^{m}** state is a near attacking conformation before **TS1^{m}**. The energy level of **R2^{m}** is higher than that of **R1^{tc}** by 3.9 kcal/mol. The apparent activation energy from **R1^{tc}** becomes 16.9 kcal/mol, which is greater than that of transesterification by 2.0 kcal/mol. This result explains the preference for transesterification over Michael addition. If we assume an Arrhenius equation, a change in the activation energy of 2.0 kcal/mol (from potential energy) at 25 °C causes selectivity of 96.7 % (99.8 % from activation free energy) toward transesterification. If we consider the optimized structure of **R2^{m}**, the structural conversion from **R1^{tt}** to **R2^{m}** involves a change in the conformation of **1a** from *s-trans* to *s-cis*. Therefore, only the *s-cis*-pathway needed to be investigated for the Michael addition. After **TS1^{m}**, the proton, which is originally at **1a**, moves to OAr (**I1^{m}**). This OAr ligand is spatially separated from the substrate. The sterically hindered OAr ligands limit the conformational rearrangement to allow direct proton transfer to the substrate. Thus, further proton transfer to another OAr ligand should be necessary (**I3^{m}**). The proton finally attacks the carbon atom to complete the reaction.

Recently, dimeric Mg(II) complexes, $[Mg(OAr)(OR)]_2$, were proposed as active species in the ring-opening polymerization (ROP) reactions.[10g] Therefore, we also considered another mechanistic possibility including such the dimeric Mg(II) complexes based on DFT calculations (Figure 6). As a result, the observed energy profiles showed that $[Mg(OAr)(OBn)]_2$ favored the transesterification pathway more than the Michael addition pathway again (See the section 18 in the SI for details). In our DFT result, dimeric Mg(II) complex is only 1.0 kcal/mol more stable than monomeric Mg(II) complex. As shown in the SI, apparent activation energy of the transesterification pathway is 1.4 kcal/mol smaller than that of the Michael addition pathway. At this preliminary stage, we cannot exclude such the reaction pathways including the dimeric Mg(II) complexes, and further mechanistic considerations based on both experiments and theoretical calculations should be necessary.

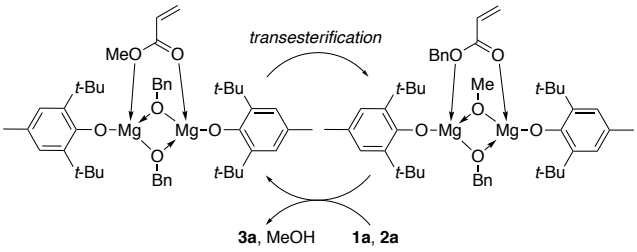

Figure 6. A possible reaction mechanism including dimeric Mg(II) complexes.

In summary, we have developed a highly chemoselective transesterification of methyl (meth)acrylates catalyzed by BHT-derived NaOAr **9** or $Mg(OAr)_2$ **10** under mild reaction conditions at 25 °C. Through extensive substrate screening, our present protocol encompassed an impressive range of functionalized primary and secondary alcohols, diols, triol, and tetraol on a scale of up to 10 mmol, leading to 2.7 g of product. Industrially useful but unstable acrylates were also obtained from glycidol, allyl alcohol, and trifluoroethanol. Moreover, preliminary transition states were proposed, and computational DFT calculations strongly supported high chemoselectivity to minimize undesired Michael additions. Overall, the observed excellent chemoselectivity, high yields, mild reaction conditions at 25 °C, and lack of any toxic metal salts make our transesterification a practical and green sustainable candidate for industrial acrylate synthesis.

ASSOCIATED CONTENT

Supporting Information

The Supporting Information is available free of charge at https://pubs.acs.org/doi/10.1021/acs.orglett.0cXXXXX.

Experimental procedures, characterization data, additional control experiments, copies of NMR spectra for all products (PDF).

AUTHOR INFORMATION

Corresponding Author

Jun-ya Hasegawa – *Section of Theoretical Catalytic Chemistry, Institute for Catalysis, Hokkaido University, N21W10, Kita-ku, Sapporo, Hokkaido 011-0021, Japan;* orcid.org/0000-0002-9700-3309; Email: hasegawa@cat.hokudai.ac.jp

Manabu Hatano – *Graduate School of Pharmaceutical Sciences, Kobe Pharmaceutical University, 4-19-1, Motoyamakitamachi, Higashinada, Kobe 658-8558, Japan;* orcid.org/0000-0002-5595-9206; Email: mhatano@kobepharma-u.ac.jp

Kazuaki Ishihara – *Graduate School of Engineering, Nagoya University, Furo-cho, Chikusa, Nagoya 464-8603, Japan;* orcid.org/0000-0003-4191-3845; Email: ishihara@cc.nagoya-u.ac.jp

Authors

Jie Qi Ng – *Graduate School of Engineering, Nagoya University, Furo-cho, Chikusa, Nagoya 464-8603, Japan*

Hiro Arima – *Graduate School of Engineering, Nagoya University, Furo-cho, Chikusa, Nagoya 464-8603, Japan*

Takuya Mochizuki – *Graduate School of Engineering, Nagoya University, Furo-cho, Chikusa, Nagoya 464-8603, Japan*

Kohei Toh – *Graduate School of Engineering, Nagoya University, Furo-cho, Chikusa, Nagoya 464-8603, Japan*

Kai Matsui – *Graduate School of Engineering, Nagoya University, Furo-cho, Chikusa, Nagoya 464-8603, Japan*

Manussada Ratanasak – *Section of Theoretical Catalytic Chemistry, Institute for Catalysis, Hokkaido University, N21W10, Kita-ku, Sapporo, Hokkaido 011-0021, Japan*

Complete contact information is available at: https://pubs.acs.org/doi/10.1021/acs.orglett.0cXXXXX.

Notes

The authors declare no competing financial interest.

ACKNOWLEDGMENT

Financial support was partially provided by JSPS KAKENHI Grant Numbers JP20H02735 (MH), JP15H05755 (KI), JP15H05810 (KI), and JP15H05805 (JH) in Precisely Designed Catalysts with Customized Scaffolding. MH is grateful for financial support from the Shorai Foundation for Science and Technology. MR and JH appreciate financial support from the Integrated Research Consortium on Chemical Sciences. Some of the computations were carried out at RCCS (Okazaki, Japan).

REFERENCES

(1) Niesbach, A.; Kuhlmann, H.; Keller, T.; Lutze, P.; Górak, A. Optimisation of industrial-scale *n*-butyl acrylate production using reactive distillation. *Chem. Eng. Sci.* **2013**, *100*, 360–372.

(2) (a) Mori, H.; Müller, A. H. E. Hyperbranched (meth)acrylates in solution, melt, and grafted from surfaces. *Top. Curr. Chem.* **2003**, *228*, 1–37. (b) Slone, R. V. Acrylic ester polymers, In *Kirk-Othmer Encyclopedia of Chemical Technology (5th Edition)*, (Ed) Seidel, A. Vol. 1, pp. 369–397, Wiley, Hoboken, **2005**.

(3) For reviews: (a) Otera, J. Transesterification. *Chem. Rev.* **1993**, *93*, 1449–1470. (b) Otera, J. *Esterification*, Wiley-VCH, Weinheim, **2003**. (c) Grasa, G. A.; Singh, R.; Nolan, S. P. Transesterification/Acylation Reactions Catalyzed by Molecular Catalysts. *Synthesis* **2004**, *2004*, 971–985. (d) Hoydonckx, H. E.; De Vos, D. E.; Chavan, S. A.; Jacobs, P. A. Esterification and Transesterification of Renewable Chemicals. *Top. Catal.* **2004**, *27*, 83–96.

(4) Recent advances in catalytic transesterification: (a) Tanaka, S.; Nakashima, T.; Satou, N.; Oono, H.; Kon, Y.; Tamura, M.; Sato, K. Epoxide as precatalyst for metal-free catalytic transesterification. *Tetrahedron Lett.* **2019**, *60*, 2009–2013. (b) Lam, Y.-P.; Wang, X.; Tan, F.; Ng, W.-H.; Tse, Y.-L. S.; Yeung, Y.-Y. Amide/Iminium Zwitterionic Catalysts for (Trans)esterification: Application in Biodiesel Synthesis. *ACS Catal.* **2019**, *9*, 8083–8092. (c) Nagae, H.; Hirai, T.; Kato, D.; Soma, S.; Akebi, S.; Mashima, K. Dinuclear manganese alkoxide complexes as catalysts for C–N bond cleavage of simple tertiary *N*,*N*-dialkylamides to give esters. *Chem. Sci.* **2019**, *10*, 2860–2868.

(5) (a) Ji, Y. Recent Development of Heterogeneous Catalysis in the Transesterification of Glycerol to Glycerol Carbonate. *Catalysts* **2019**, *9*, 581/1–581/22. (b) Zhang, H.; Lia, H.; Hu, Y.; Rao, K. T. V.; Xu, C.; Yang, S. Advances in production of bio-based ester fuels with heterogeneous bifunctional catalysts. *Renew. Sust. Energ. Rev.* **2019**, *114*, 109296. (c) Gupta, J.; Agarwal, M.; Dalai, A. K. An overview on the recent advancements of sustainable heterogeneous catalysts and prominent continuous reactor for biodiesel production. *J. Ind. Eng. Chem.* **2020**, *88*, 58–77.

(6) (a) Salinier, V.; Niccolai, G. P.; Dufaud, V.; Basset, J.-M. Silica-Supported Zirconium Complexes and their Polyoligosilsesquioxane Analogues in the Transesterification of Acrylates: Part 2. Activity, Recycling and Regeneration. *Adv. Synth. Catal.* **2009**, *351*, 2168–2177. (b) Gaudino, M. C.; Valentin, R.; Brunel, D.; Fajula, F.; Quignard, F.; Riondel, A. Titanium-based solid catalysts for transesterification of methyl-methacrylate by 1-butanol: the homogeneous catalysis contribution. *Appl. Catal. A: Gen.* **2005**, *280*, 157–164. (c) Baquey, G.; Alvès, M.-H.; Graullier, M.; Riondel, A.; Paul, J.-M.; Birot, M.; Deleuze, H. An efficient, practical and cost-effective polymer-supported catalyst for the transesterification of methyl methacrylate by 1-butanol. *Green Chem.* **2009**, *11*, 868–872. (d) Adriana, M.; Nadine, E.; Lorraine, C.; François, F. Transesterification of acrylates by heterogeneous basic catalysis. *Appl. Catal. A: Gen.* **2013**, *468*, 1–8.

(7) (a) Ohshima, T.; Iwasaki, T.; Maegawa, Y.; Yoshiyama, A.; Mashima, K. Enzyme-Like Chemoselective Acylation of Alcohols in the Presence of Amines Catalyzed by a Tetranuclear Zinc Cluster. *J. Am. Chem. Soc.* **2008**, *130*, 2944–2945. (b) Iwasaki, T.; Maegawa, Y.; Hayashi, Y.; Ohshima, T.; Mashima, K. Transesterification of Various Methyl Esters Under Mild Conditions Catalyzed by Tetranuclear Zinc Cluster. *J. Org. Chem.* **2008**, *73*, 5147–5150. (c) Iwasaki, T.; Maegawa, Y.; Hayashi, Y.; Ohshima, T.; Mashima, K. A Simple, General, and Highly Chemoselective Acetylation of Alcohols Using Ethyl Acetate as the Acetyl Donor Catalyzed by a Tetranuclear Zinc Cluster. *Synlett* **2009**, *2009*, 1659–1663. (d) Iwasaki, T.; Agura, K.; Maegawa, Y.; Hayashi, Y.; Ohshima, T.; Mashima, K. *Chem. Eur. J.* **2010**, *16*, 11567–11571. (e) Hayashi, Y.; Ohshima, T.; Fuji, Y.; Matsushima, Y.; Mashima, K. A trifluoroacetic acid adduct of a trifluoroacetate-bridged μ_4-oxo-tetranuclear zinc cluster, $Zn_4(OCOCF_3)_6O{\cdot}CF_3CO_2H$: synthesis under mild conditions and catalytic transesterification and oxazoline formation. *Catal. Sci. Technol.* **2011**, *1*, 230–233. (f) Maegawa, Y.; Ohshima, T.; Hayashi, Y.; Agura, K.; Iwasaki, T.; Mashima, K. *ACS Catal.* **2011**, *1*, 1178–1182. (g) Maegawa, Y.; Agura, K.; Hayashi, Y.; Ohshima, T.; Mashima, K. Transesterification of α-Amino Esters Catalyzed by a Tetranuclear Zinc Cluster: $Zn_4(OCOCF_3)_6O$. *Synlett* **2012**, *23*, 137–141.

(8) Nakatake, D.; Yazaki, R.; Ohshima, T. Chemoselective Transesterification of Acrylate Derivatives for Functionalized Monomer Synthesis Using a Hard Zinc Alkoxide Generation Strategy. *Eur. J. Org. Chem.* **2016**, 3696–3699.

(9) Hatano, M.; Tabata, Y.; Yoshida, Y.; Toh, K.; Yamashita, K.; Ogura, Y.; Ishihara, K. Metal-free transesterification catalyzed by tetramethylammonium methyl carbonate. *Green Chem.* **2018**, *20*, 1193–1198.

(10) (a) Calvo, B.; Davidson, M. G.; García-Vivó, D.; Polyamine-Stabilized Sodium Aryloxides: Simple Initiators for the Ring-Opening Polymerization of *rac*-Lactide. *Inorg. Chem.* **2011**, *50*, 3589–3595. (b) Fang, H.-J.; Lai, P.-S.; Chen, J.-Y.; Hsu, S. C. N.; Peng, W.-D.; Ou, S.-W.; Lai, Y.-C.; Chen, Y.-J.; Chung, H.; Chen, Y.; Huang, T.-C.; Wu, B.-S.; Chen, H.-Y. ε-Caprolactone polymerization under air by the

biocatalyst: Magnesium 2,6-di-*tert*-butyl-4-methylphenoxide. *J. Polym. Sci. Part A: Polym. Chem.* **2012**, *50*, 2697–2704. (c) Chen, H.-Y.; Mialon, L.; Abboud, K. A.; Miller, S. A. Comparative Study of Lactide Polymerization with Lithium, Sodium, Magnesium, and Calcium Complexes of BHT. *Organometallics* **2012**, *31*, 5252–5261. (d) Wilson, J. A.; Hopkins, S. A.; Wright, P. M.; Dove, A. P. 'Immortal' ring-opening polymerization of ω-pentadecalactone by $Mg(BHT)_2(THF)_2$. *Polym. Chem.* **2014**, *5*, 2691–2694. (e) Wilson, J. A.; Hopkins, S. A.; Wright, P. M.; Dove, A. P. Synthesis of ω-Pentadecalactone Copolymers with Independently Tunable Thermal and Degradation Behavior. *Macromolecules* **2015**, *48*, 950–958. (f) Nifant'ev, I. E.; Shlyakhtin, A. V.; Tavtorkin, A. N.; Ivchenko, P. V.; Borisov, R. S.; Churakov, A. V. Monomeric and dimeric magnesium mono-BHT complexes as effective ROP catalysts. *Catal. Commun.* **2016**, *87*, 106–111. (g) Nifant'ev, I. E.; Shlyakhtin, A. V.; Bagrov, V. V.; Minyaev, M. E.; Churakov, A. V.; Karchevsky, S. G.; Birin, K. P.; Ivchenko, P. V. Mono-BHT heteroleptic magnesium complexes: synthesis, molecular structure and catalytic behavior in the ring-opening polymerization of cyclic esters. *Dalton Trans.* **2017**, *46*, 12132–12146.

(11) Rappoport, Z. *The Chemistry of Phenols.* John Wiley & Sons, Chichester, **2003**.

(12) Benjamin, B. M.; Raaen, V. F.; Hagaman, E. W.; Brown, L. L. Some unusual oxidation products of 2,6-di-*tert*-butyl-4-methylphenol. *J. Org. Chem.* **1978**, *43*, 2986–2991. (b) Omura, K. Reinvestigation of the reaction of 2,6-di-*tert*-butylbenzoquinone methide and 2,6-di-*tert*-butylphenol. *J. Org. Chem.* **1992**, *57*, 306–312. (c) Gamez, P. Phenol Oxidations. In *Liquid Phase Aerobic Oxidation Catalysis: Industrial Applications and Academic Perspectives.* (Eds.) Shannon, S. S.; Alsters, P. L. Cp. 7, pp. 97–109, John Wiley-VCH, Weinheim, **2016**.

(13) In this regard, the US FDA (Food and Drug Administration) approved BHT as a safe food additive and preservative in 1954. Fujisawa, S.; Kadoma, Y.; Yokoe, I. Radical-scavenging Activity of Butylated Hydroxytoluene (BHT) and Its Metabolites. *Chem. Phys. Lipids* **2004**, *130*, 189–195.

(14) For review: (a) Bartsch, R.; Drost, C.; Klingebiel, U. Organometallic and inorganic compounds of the alkali and alkaline earth metals. In *Synthetic Methods of Organometallic and Inorganic Chemistry*, (Eds.) Auner, N.; Klingebiel, U. pp. 1–62, Thieme, Stuttgart, **1996**. (b) North, M. (Ed.) *Sustainable Catalysis: With Non-endangered Metals.* Royal Society of Chemistry, Cambridge, **2016**.

(15) The diversity of inexpensive and commercially available phenol-analogous to BHT prompted us to consider the effect of substituents on the phenoxide moiety. As a result, BHT-derived salts (i.e., **9** and **10**) were much better than others. See the Supporting Information.

(16) (a) Seebach, D.; Hungerbühler, E.; Naef, R.; Schnurrenberger, P.; Weidmann, B.; Züger, M. *Synthesis* **1982**, *1982*, 138–141. (b) Krasik, P. Synthesis of sterically hindered esters via titanium catalyzed transesterification. *Tetrahedron Lett.* **1998**, *39*, 4223–4226.

(17) Weng, S.-S.; Ke, C.-S.; Chen, F.-K.; Lyu, Y.-F.; Lin, G.-Y. Transesterification catalyzed by iron(III) β-diketonate species. *Tetrahedron* **2011**, *67*, 1640–1648.

(18) (a) Okano, T.; Miyamoto, K.; Kiji, J. Transesterification Catalyzed by Lanthanoid Tri-2-propoxides. *Chem. Lett.* **1995**, *24*, 246-246. (b) Neverov, A. A.; Brown, R. S. Catalysis of the methanolysis of acetylimidazole by lanthanum triflate. *Can. J. Chem.* **2000**, *78*, 1247–1250. (c) Hatano, M.; Furuya, Y.; Shimmura, T.; Moriyama, K.; Kamiya, S.; Maki, T.; Ishihara, K. Ligand-Assisted Rate Acceleration in Lanthanum(III) Isopropoxide Catalyzed Transesterification of Carboxylic Esters. *Org. Lett.* **2011**, *13*, 426–429. (d) Hatano, M.; Kamiya, S.; Moriyama, K. Ishihara, K. Lanthanum(III) Isopropoxide Catalyzed Chemoselective Transesterification of Dimethyl Carbonate and Methyl Carbamates. *Org. Lett.* **2011**, *13*, 430–433. (e) Hatano, M.; Kamiya, S.; Ishihara, K. In situ generated "lanthanum(III) nitrate alkoxide" as a highly active and nearly neutral transesterification catalyst. *Chem. Commun.* **2012**, *48*, 9465–9467.

(19) Malshe, V. C.; Vaidya, M. S. Acrylic functional monomers. Part I. *Paintindia* **1995**, *45*, 33–42.

(20) (a) Bywater, S.; Black, P. E.; Wiles, D. M. The anionic polymerization of allyl acrylate and allyl methacrylate. *Can. J. Chem.* **1966**, *44*, 695–702. (b) Druzhinina, T. V. Sorptive polymers based on modified fibers. *Fibre. Chem.* **2012**, *44*, 204–209. (c) Tanaka, S.; Nakashima, T.; Maeda, T.; Ratanasak, M.; Hasegawa, J.; Kon, Y.; Tamura, M.; Sato, K. Quaternary Alkyl Ammonium Salt-Catalyzed Transformation of Glycidol to Glycidyl Esters by Transesterification of Methyl Esters. *ACS Catal.* **2018**, *8*, 1097–1103.

(21) (a) Suzuki, A.; Fujiwara, M.; Nishijima, M. High spin/low spin phase transitions of a spin-crossover complex in the emulsion polymerization of trifluoroethylmethacrylate (TFEMA) using PVA as a protective colloid. *Colloid Polym. Sci.* **2008**, *286*, 525–534. (b) Ziegert, F.; Koof, M.; Wagner, J. A new class of co-polymer colloids with tunable, low refractive index for investigations of structure and dynamics in concentrated suspensions. *Colloid Polym. Sci.* **2017**, *295*, 1563–1574.

(22) (a) De Vries, T. S.; Goswami, A.; Liou, L. R.; Gruver, J. M.; Jayne, E.; Collum, D. B. Lithium Phenolates Solvated by Tetrahydrofuran and 1,2-Dimethoxyethane: Structure Determination Using the Method of Continuous Variation. *J. Am. Chem. Soc.* **2009**, *131*, 13142–13154. (b) Boyle, T. J.; Velazquez, A. T.; Yonemoto, D. T.; Alam, T. M.; Moore, C.; Rheingold, A. L. Synthesis and characterization of a family of solvated sodium aryloxide compounds. *Inorg. Chim. Acta* **2013**, *405*, 374–386. (c) Calabrese, J.; Cushing, Jr. M. A.; Ittel, S. D. Sterically hindered magnesium aryloxides. *Inorg. Chem.* **1988**, *27*, 867–870. (d) Zechmann, C. A.; Boyle, T. J.; Rodriguez, M. A.; Kemp, R. A. Synthesis, characterization, and structural study of sterically hindered magnesium alkoxide and siloxide compounds. *Inorganica Chim. Acta* **2001**, *319*, 137–146.

(23) FAB-MS analysis of **9** and **10** revealed the predominance of the respective monomers. Moreover, ^{1}H NMR study showed that proton exchange from **9**/**2a** to ArOH/BnONa is unlikely, and therefore **9** would be almost intact under the reaction conditions. See the Supporting Information.

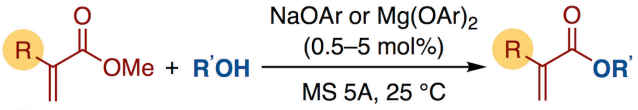

R = Me, H; ArOH = BHT

- √ *1° and 2°-Alcohols, diol, triol, tetraol*
- √ *High chemoselectivity*
- √ *High yield*
- √ *Room temperature operation*
- √ *No toxic metal or ligand*